Research Article

Imaging of type I procollagen biosynthesis in cells reveals biogenesis in highly organized bodies; Collagenosomes

Branko Stefanovic [a*], **Lela Stefanovic** [a] **and Zarko Manojlovic** [b]

***a* - Department of Biomedical Sciences and Translational Science Laboratory,** *College of Medicine, Florida State University, 1115 West Call Street, Tallahassee, FL 32306, USA*

***b* - Keck School of Medicine of University of Southern California,** *1450 Biggy Street, NRT 4510, Los Angeles, CA 90033, USA*

Correspondence to Branko Stefanovic: *branko.stefanovic@med.fsu.edu (B. Stefanovic)*
https://doi.org/10.1016/j.mbplus.2021.100076

Abstract

Mechanistic aspects of type I procollagen biosynthesis in cells are poorly understood. To provide more insight into this process we designed a system to directly image type I procollagen biogenesis by co-expression of fluorescently labeled full size procollagen α1(I) and one α2(I) polypeptides. High resolution images show that collagen α1(I) and α2(I) polypeptides are produced in coordination in discrete structures on the ER membrane, which we termed the collagenosomes. Collagenosomes are disk shaped bodies, 0.5–1 μM in diameter and 200–400 nm thick, in the core of which folding of procollagen takes place. Collagenosomes are intimately associated with the ER membrane and their formation requires intact translational machinery, suggesting that they are the sites of nascent procollagen biogenesis. Collagenosomes show little co-localization with the COPII transport vesicles, which export type I procollagen from the ER, suggesting that these two structures are distinct. LARP6 is the protein which regulates translation of type I collagen mRNAs. The characteristic organization of collagenosomes depends on binding of LARP6 to collagen mRNAs. Without LARP6 regulation, collagenosomes are poorly organized and the folding of α1(I) and α2(I) polypeptides into procollagen in their cores is diminished. This indicates that formation of collagenosomes is dependent on regulated translation of collagen mRNAs. In live cells the size, number and shape of collagenosomes show little change within several hours, suggesting that they are stable structures of type I procollagen biogenesis. This is the first report of structural organization of type I collagen biogenesis in collagenosomes, while the fluorescent reporter system based on simultaneous imaging of both type I collagen polypeptides will enable the detailed elucidation of their structure and function.

Introduction

Type I collagen is the most abundant protein in human body [1]. It is composed of two polypeptides, α1(I) and α2(I), where two α1(I) and α2(I) polypeptides fold into triple helix. The biogenesis of type I collagen involves multiple steps [2]. Collagen mRNAs are translated on the membrane of the endoplasmic reticulum (ER) and nascent polypeptides are inserted into the lumen. The nascent polypeptides undergo isomerization of Gly-Pro bonds [3,4], hydroxylations of selected prolines and lysines [5] and glycosylations of hydroxylysines [6]. Two α1(I) polypeptides and one α2(I) polypeptide register at the C-terminal ends and disulfide bond, forming the nucleation center for folding of the polypeptides into triple helix in a zipper-like fashion from the C-terminus to the N-terminus [7–13]. Molecular chaperones facilitate these processes [14,15] and the folded helices are packed into COPI II vesicles by TANGO1 chaperone for export from the ER to Golgi and outside of

the cell [16–18]. It is believed that these events take place in the lumen of the ER.

In tissues type I collagen is always a heterotrimer of two α1(I) and one α2(I) polypeptides, although α1 (I) polypeptides have a propensity to form homotrimers. This was observed in rare individuals who have complete absence of α2(I) polypeptide [19] and in animals in which expression of α2(I) gene was knocked out [20]. Homotrimers are less stable, but they are functional [21], resulting in a phenotype of Ehlers-Danlos syndrome. However, in normal tissues type I collagen is always present as the heterotrimer, suggesting that there is a mechanism which favors the formation of heterotrimers over α1(I) homotrimers.

The abundance of type I collagen in tissues is primarily due to the slow turnover of collagen fibers. The half-life of collagen in tissues was estimated to be in years [22,23]. Type I collagen has fractional synthesis rate (FSR, % synthesis per hour) in collagen rich tissues of 0.018–0.045 $\%h^{-1}$ [24,25]. However, in the pathological state of fibrosis the FSR of type I collagen in tissues that normally produce only small amounts increases significantly. For example, in normal liver the FSR is $0.008\%h^{-1}$, while in fibrotic liver it is $0.025\%h^{-1}$ [26]. To accommodate the high biosynthetic rate of type I procollagen in fibrosis a mechanism that increases the efficacy of type I procollagen biogenesis must be activated. This mechanism is not critical for the constitutive type I collagen biosynthesis, but is needed to sustain the higher biosynthetic rate [27]. It is initiated by binding of the RNA binding protein LARP6 to mRNAs encoding for type I and type III collagens [28–31]. LARP6 binds the unique sequence in the 5′UTR of these mRNAs, which folds into a structure composed of two stems flanking the central bulge and was termed the collagen 5′ stem-loop (5′SL). By binding 5′SL of type I collagen mRNAs, LARP6 acts as an adapter protein to recruit accessory translational factors, which increase translational competency of collagen mRNAs and coordinate translation of collagen α1 (I) and α2(I) mRNAs [32–34]. LARP6 may also regulate translation of type III collagen mRNA, but this has not been studied. Because type I collagen is the major collagen in fibrosis, an animal model was developed to study the role of LARP6 in type I collagen regulation. Mice in which binding of LARP6 to the 5′SL of collagen α1(I) mRNA was abolished were resistant to development of liver fibrosis [27]. These animals develop normally, suggesting that LARP6 regulation controls only the accelerated type I collagen production in fibrosis. This led to the hypothesis that inhibitors of LARP6 binding to collagen mRNAs can act as specific antifibrotic drugs [35]. Two such inhibitors have already been discovered [36,37].

In this work we show that biogenesis of type I collagen takes place on the membrane of the ER in distinct bodies, which we termed the collagenosomes. Formation of collagenosomes is dependent on the integrity of translational machinery and on function of LARP6. This is the first report to demonstrate that biogenesis of type I collagen is organized in discrete structures and associated with the ER membrane.

Materials and methods

Construction of reporter genes expressing fluorescently labeled collagen polypeptides. For construction of A1-BFP reporter gene full size human collagen α1(I) cDNA in clone X07884 (ATCC 95498) was cut with EcoRI and 4.5 kb fragment was cloned into EcoRI site of pCDNA3 vector. AgeI site was created at codon 26 by site directed mutagenesis using the following primers; GGCCAAGAGGAAGGACCGGTCGAGGGCCAA GA and TCTTGGCCCTCGAC CGGTCCTTCCTC TTGGCC. The cDNA of mTagBFP2 protein was PCR amplified with primers: GCCACCGGTAGTG TCTAAGGGCGAAGAGCT and GCCACCGGTGC ACCTCCGCC CCCATTAAGCTTGTGCCCCAGTT, cut with AgeI and cloned into the AgeI site of the above pCDNA3 construct. Full size collagen α1(I) cDNA was recreated by appending the ClaI-HindIII fragment from X07884 into this last clone, creating the A1-BFP reporter in pCDNA3 vector.

For making adenovirus expressing A1-BFP reporter, pAdTrack-CMV vector was modified by removing the HpaI fragment (containing the GFP cassette) and religating the vector. The NotI-SalI fragment of the A1-BFP/pCDNA3 construct was recloned into NotI and XhoI of the modified pAdTrack-CMV vector. Adenovirus was assembled by recombination of this clone with pAdEasy in BJ5 183 E. coli cells and packaged in HEK293 cells and amplified using the standard procedures [38].

For construction of A2-GFP and A2Δ5′SL-GFP reporter genes full size human collagen α2(I) cDNA in clone BC042586 (MGC:30044 IMAGE:4803351) was shortened by cutting with XcmI and HindIII, removing the fragments and religating the clone after blunting the ends. For making A2-GFP, double stranded oligonucleotide with sequence TCAGCTTTGTGGATACGCGGA CTT TGTTGCTGCTTGCAGTAACCTTATGCCTA GCAACATGCCAATCTTTACAAGAGGATCCTGT AAGAAAGGGCC was ligated into BplI and ApaI sites of the truncated collagen α2(I) cDNA. For making A2Δ5′SL-GFP, double stranded oligonucleotide with sequence TCACGTTCGTAG ATACGCGGAC TTTGTTGCTGCTTGCAGTAAC CTTATGCCTAGCAACATGCCAATCTTTACAAGA GGATCCTGTAAGAAAGGGCC was cloned into BplI and ApaI sites. cDNA for Emerald GFP protein was amplified by PCR with primers: CGCAGATCTAGTGAGCAAGGGCGAGGAGCT and CGCAGATCTCCACCTCC GCCCTTGTA

CAGCTCGTCCA TGCC, the PCR product was cut with BglII and ligated into BamHI site of the above A2-GFP and A2Δ5′SL-GFP constructs. The KpnI and PmlI fragment was cut from these clones and ligated back into KpnI-PmlI sites of BC042586, creating A2-GFP and A2Δ5′SL-GFP reporters in pSPORT vector.

For making adenoviruses expressing A2-GFP and A2Δ5′SL-GFP, KpnI-NotI fragment from pSPORT vectors was recloned into KpnI and NotI sites of the modified pAdTrack-CMV vector and adenoviruses were assembled as described above.

Cell culture and immunostaining. Human lung fibroblasts (HLFs) and hepatic stellate cells (HSCs) were described before [39,40]. Scleroderma fibroblasts were from European Collection of Cell Cultures (ECACC), cell line BM0070. The cells were cultured under standard conditions in DMEM supplemented with 10% fetal calf serum.

CRISPR-Cas9 knock down of LARP6 in HLFs was done using pCas9GFP vector (addgene #48138) expressing the sgRNA targeting LARP6 with sequence: CGGATCTGCACCGCCGTCTT GGG, quality score 93, 9 off-target sites with score of 0.9 [41]. The vector was transfected into HLFs and individual clones were selected by cell sorting and LARP6 expression verified by western blot.

For immunostaining, the cells were seeded onto glass coverslips and grown to 50% confluency, when they were fixed in 4% formaldehyde in PBS for 10 min. Cells were permeabilized with 0.1% Triton X-100 in PBS for 10 min and blocked with 1% bovine serum albumin for 2 h, followed by incubation with the following antibodies: anti-collagen antibody (Rockland 600–401-103), anti-α2(I) antibody (Santa Cruz Biotechnology sc-8786), anti-COPII antibody (Invitrogen PA1-069A) and anti-calnexin antibody (BD Transduction Laboratories 611346) at 4 °C overnight. For negative control the primary antibodies were omitted. After washing, the fluorescent-conjugated secondary antibodies were added and incubated at room temperature for 1 h. Cells were mounted with Prolong mounting solution with or without 4′, 6′-diamidino-2-phenylindole (DAPI) (Invitrogen).

For imaging fluorescent collagen reporters, adenoviruses expressing A1-BFP and A2-GFP or A2-Δ5′SL GFP reporters were added to the cells on cover slips in ratio of 2:1 and incubated for 2 days. The cells were fixed in 4% formaldehyde, mounted and imaged.

Purification of microsomes. Microsomal fraction was prepared as reported before [42], with minor modifications [43]. Cells were resuspended in 0.5 ml of hypotonic buffer and homogenized in Dounce Homogenizer. The homogenate was mixed with 2 ml of 2.5 M sucrose and overlaid with 2 ml of 1.9 M and 1.3 M sucrose and centrifuged at 260,000×*g* for 3 h at 4 °C. The band at the 1.3 M/1.9 M sucrose interface was recovered and centrifuged in a Beckman TLA120.2 rotor at 66,000×*g* for 20 min at 4 °C. Microsomes in the pellet were resuspended in 25 mM Hepes, pH7.2, 150 mM KAc, 5 mM MgAc and used for Western blot or fixed by adding glutaraldehyde to 0.15% and mounted with Prolong mounting solution onto coverslips for direct imaging. In some experiments digitonin was added to the resuspension buffer to 3.5% and microsomes were lysed by incubation on ice for 10 min prior to fixing and mounting. For immunostaining, resuspended microsomes were spotted on poly-L lysine coated coverslips, fixed with 0.15% glutaraldehyde and immunostained with anti-collagen antibody as described for cells.

Western blots. Antibodies used were: anti-LARP6 antibody from Abnova (H00055323-B01P), anti-collagen α1(I) antibody from Rockland (600–401-103), anti-calnexin and anti-golgin antibody from BD Transduction Laboratories (611346 and 611382), anti-β-actin antibody from Abnova (ab8227), anti-GAPDH antibody from Millipore-Sigma (ABS16) and anti-GFP antibody from Sigma (G6539).

Typically, 40 μg of total cellular protein was used for Western blotting analysis. Proteins were resolved on 7.5% SDS-PAGE gels, transferred onto nitrocellulose membrane and probed with 1:1000 dilution of primary antibodies. For western blots under nonreducing conditions proteins were resolved on 4% SDS-PAGE gels without adding mercaptoethanol or DTT to the samples. For western blotting analysis of cellular medium proteins, the cells were grown in 6-well plates to 80% confluency, washed 3 times with serum free medium and 200 μL of serum free medium was added per well. This medium was incubated for 3 h, collected, and 50–100 μL was directly analyzed by Western blotting.

Imaging of cells and microsomes. Two imaging systems were used; the OMX Deltavision V4 system with structured illumination module and the Keyence BZ-X710 microscope with optical sectioning module, as indicated in the figure legends. Some control images were also taken with EVOS FL microscope, as indicated. Live cell imaging was done by Andor Dragonfly 505 confocal imaging system. The images were taken at 60x magnification and the higher magnification of 3D microsomes was obtained by applying 3x zoom. For reconstruction of 3D images, confocal images were arranged in stacks and 3D view was constructed using Image J software.

For quantification of fluorescence overlap in fixed cells, areas containing collagenosomes were selected and cyan pixels (overlap of blue and green pixels) and green pixels were counted in the same area using Color Pixel Counter plugin of Image J. The number of cyan pixels was normalized to number of green pixels and expressed as percentage overlap.

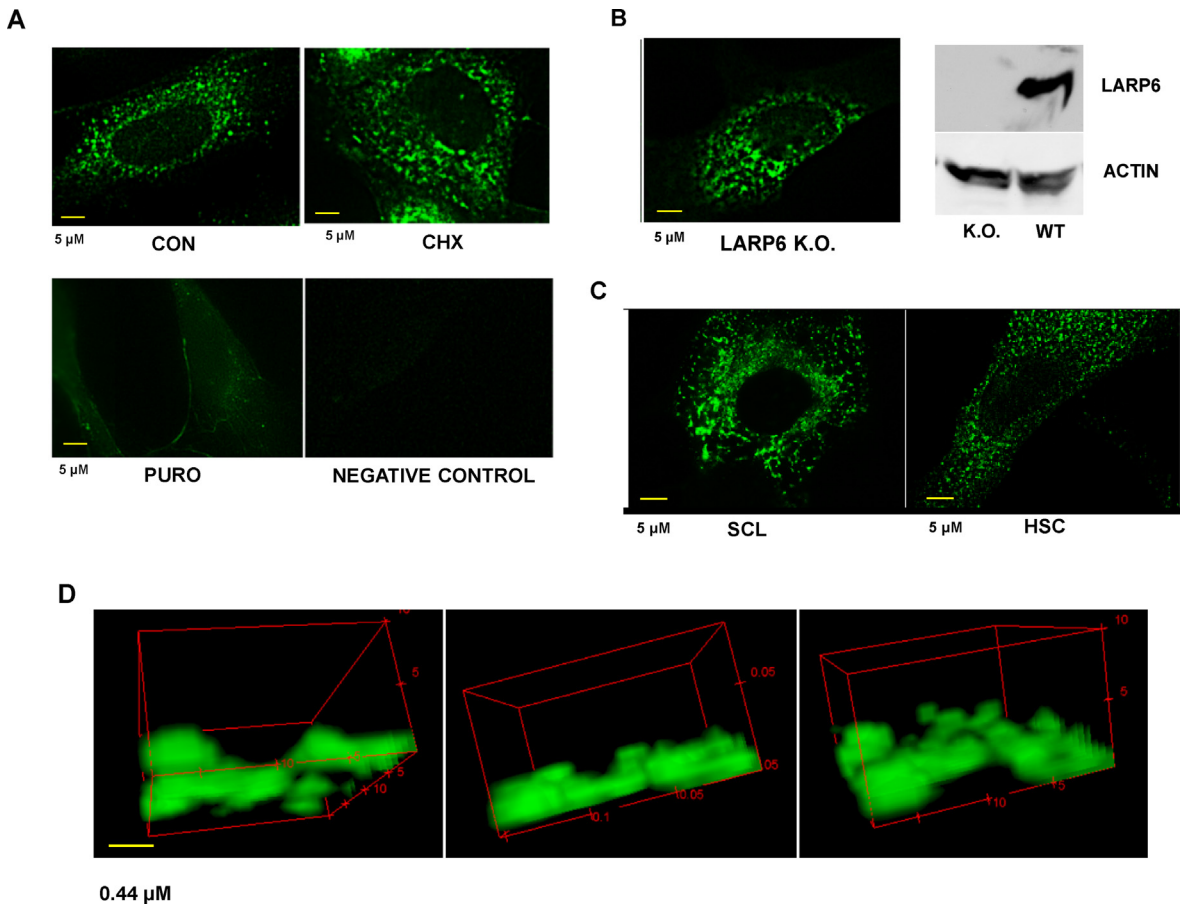

Fig. 1. Subcellular localization of type I procollagen in human lung fibroblasts (HLFs). A. Immunostaining of type I procollagen in wt HLFs. Upper left panel: untreated wt HLFs (CON), upper right panel: HLFs treated with cycloheximide for 1 h (CHX), lower left panel: HLFs treated with puromycin for 1 h (PUR), lower right panel: negative control staining, (Keyence BZ-X710). B. Immunostaining of type I procollagen in LARP6 knock out HLFs. Left panel: immunostaining in LARP6 knock out HLFs (LARP6 K.O.), (Keyence BZ-X710), right panel: western blot of LARP6 and actin in LARP6 knock out HLFs (K.O.) and wt HLFs (WT). C. Immunostaining of type I procollagen in scleroderma fibroblasts (SCL) and human hepatic stellate cells (HSCs), (Keyence BZ-X710). D. 3D image of collagenosomes in immunostained HLF. Three different angles of view of the same group of collagenosomes is shown. The image was reconstructed from 11 confocal images, (OMX Deltavision V4).

Results

Biosynthesis of type I procollagen in fibroblasts is localized to discrete spots in the perinuclear region. The cells used in this study were pulmonary and dermal fibroblasts and hepatic stellate cells. In in vivo fibrosis these cells become activated and increase type I procollagen production. When these cells are cultured in vitro they assume their activated phenotype [44 45,46]. Therefore, by using cultured cells our results pertain to the type I procollagen biogenesis in the cells with high biosynthetic rate.

If the intracellular localization of type I procollagen is visualized by immunostaining of cells, the image will display the localization at the time of fixation of cells. Because procollagen is a secreted protein, the intracellular accumulation will display the equilibrium between these two processes. Fig. 1A, upper left panel, shows that in human lung fibroblasts (HLFs), the cells responsible for pulmonary fibrosis, type I procollagen accumulated in discrete perinuclear foci. When the cells were treated with cycloheximide, which inhibits translation but preserves the integrity of polysomes [47], the focal pattern of accumulation was preserved (upper right panel). However, when polysomes were dissociated with puromycin, which dissociates polysomes [48], the procollagen signal was greatly diminished and the foci disappeared (lower left panel). This indicated that the focal pattern of intracellular procollagen accumulation is dependent on the integrity of translational machinery and that it displays the sites at which procollagen polypeptides are translated.

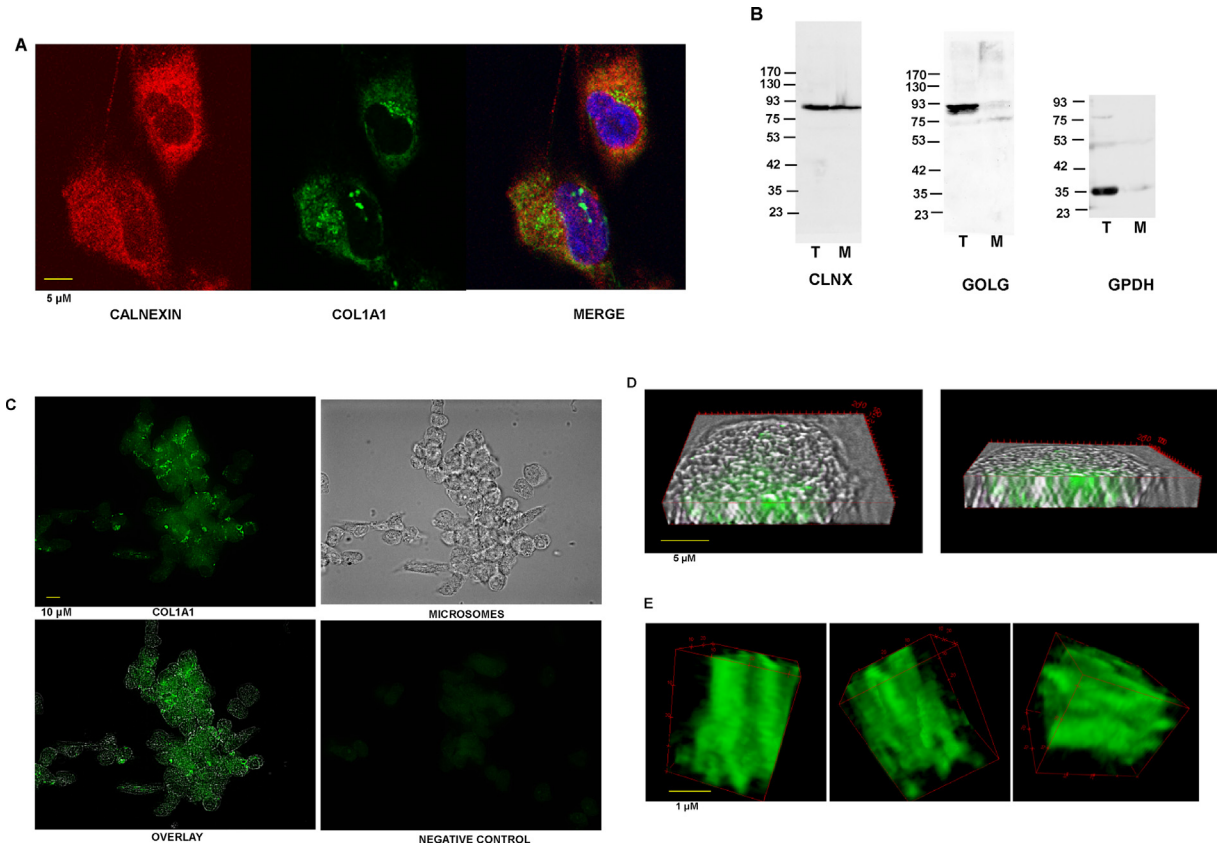

Fig. 2. Collagenosomes form on the endoplasmic reticulum (ER) membrane. A. Immunostaining of HLFs for calnexin (left panel), type I procollagen (COL1A1, middle panel) and the merged image (right panel), (Evos FL). B. Western blot for calnexin (CLNX), golgin 83 (GOLG) and GAPDH (GPDH) in total cell lysate of HLFs (T) and in purified microsomes (M). C. Immunostaining of type I procollagen in HLFs microsomes. Upper left panel: immunostaining of type I procollagen (COL1A1), upper right panel: phase contrast image of microsomes, lower left panel: overlaid image, lower right panel: negative control for immunostaining, (Keyence BZ-X710). D. 3D image of microsomes. 36 of 0.1 μM thick confocal sections of microsomes immunostained for type I procollagen (green) and phase contrast images of the same sections were overlaid and reconstructed in 3D. Two angles of view of the same microsome is shown (Keyence BZ-X710). E. Enlarged view of procollagen immunostaining in microsomes. 42 confocal sections of microsomes immunostained for type I procollagen were zoomed 3x and reconstructed in 3D, (Keyence BZ-X710). (For interpretation of the references to color in this figure legend, the reader is referred to the web version of this article.)

LARP6 is the protein which regulates translation of type I collagen mRNAs [32,49]. To assess if LARP6 plays a role in regulating the focal pattern of type I collagen translation, we knock down LARP6 expression in HLFs by CRISPR-Cas9 method and immunostained the cells (Fig. 1B). In a LARP6 knock out cell the procollagen foci were less numerous and coalesced into larger bodies which aggregated around the nucleus. This is clearly discerned in the surface plots of the WT cell (from Fig. 1A upper left panel) and the LARP6 K.O. cell (from Fig. 1B, left panel), what is shown in supplemental Fig. 1. This suggested that LARP6 regulatory activity is necessary for the formation of biosynthetic foci.

To verify that other collagen producing cells show similar focal pattern of intracellular type I procollagen, we immunostained the endogenous type I procollagen in human scleroderma skin fibroblasts and in human hepatic stellate cells (HSCs), these cells are responsible for dermal and hepatic fibrosis, respectively (Fig. 1C). Both cell types showed type I collagen biosynthesis in discrete foci, indicated that it is a general phenotype of the collagen producing cells responsible for fibrosis, and we termed these foci the collagenosomes.

To provide some structural detail of collagenosomes we reconstructed their 3D images from 11 high resolution confocal slices of the immunostained HLFs. These images were obtained by OMX DeltaVision microscope equipped with four cameras to capture the spatial outline. Fig. 1D shows three different angles of a group of collagenosomes. Most collagenosomes appeared as disk shaped bodies with diameter of

0.5–1 μM and thickness of 200–400 nM. Some collagenosomes appeared smaller, what may be an artifact of nonuniform binding of the antibody used for immunostaining.

Endoplasmic reticulum (ER) membrane as the platform for collagenosomes formation. Perinuclear localization of collagenosomes and their dependence on the integrity of polysomes suggested that they form at the ER membrane. When immunostaining of type I procollagen was overlaid with immunostaining of calnexin, an integral protein of the ER membrane, it was clear that the collagenosomes did not spread beyond the calnexin signal (Fig. 2A), suggesting that they are confined to the ER. Supplemental Fig. 2 shows that calnexin immunostaining was restricted to the perinuclear space and not spread to the periphery of cells, outlining the ER.

To further verify their localization to the ER membrane we purified microsomes, the vesicles which form after disruption of intracellular membranes and which predominantly contain the ER membranes. To assess the purity of microsomes we analyzed the preparation for presence of calnexin, as the ER membrane marker, and for absence of golgin 83 and GAPDH, as Golgi and cytosolic markers, respectively (Fig. 2B). In our microsomal preparations calnexin was present in the amount equivalent to that in whole cell extract, while only tracing amounts of golgin 83 and GAPDH were found. Therefore, we fixed microsomes with glutaraldehyde and immunostained the preparation with anti-collagen antibody. Fig. 2C, upper left panel shows confocal image of type I procollagen immunostaining in the microsomes, while upper right panel shows the phase contrast image. From the phase contrast image, the average size of microsomes was estimated to be 16 + -2.5 μM. The overlaid image (lower left panel) shows that the focal pattern of type I procollagen accumulation was preserved in the microsomes, suggesting that collagenosomes copurify with the ER membranes.

To provide 3-dimensional reconstruction of collagenosomes imbedded in the microsomal membranes we obtained 36 confocal slices and arranged them in a stack. Fig. 2D shows two angled views of a microsomal vesicle (gray), with procollagen staining (green) imbedded between the folds of membranes. This is an additional demonstration of the intimate association of type I procollagen with the ER membrane.

We also reconstructed the 3D image of procollagen in the microsomal membranes after immunostaining, but without obscuring these images with the phase contrast of microsomes. Fig. 2E shows three angles of view of one such structure. Procollagen appeared in cylindrical structures, as imbedded between the membrane sheets.

Collagenosomes and COPII vesicles are distinct structures. COPII containing vesicles assemble on the ER membrane and transport procollagen molecules from to the ER to the Golgi complex [16,50]. To demonstrate that collagenosomes are distinct from the COPII containing vesicles we co-immunostained procollagen α2(I) polypeptide and COPII in HLFs and overlaid the images (Fig. 3). The negative controls of procollagen α2(I) and COPII immunostaining is shown in supplemental Fig. 3. From Fig. 3 it is clear that the majority of procollagen α2(I) polypeptide, as the marker of collagenosomes (red), and COPII protein, as the marker of COPII vesicles (green) are segregated (overlaid image and inset in Fig. 3). Some collagenosomes and COPII vesicles showed colocalization (yellow), indicated that biogenesis and export of type I procollagen molecules may be coupled in limited number of instances.

To demonstrate the spatial positioning of collagenosomes relative to the COPII vesicles, we reconstructed the 3D images from 11 high resolution confocal slices of the co-immunostained cells using OMX DeltaVision microscope (Fig. 3B). From the three different angles of view of a group of vesicles it is clear that the majority of collagenosomes (red) and COPII vesicles (green) are spatially segregated, although some particles showed partial overlap.

This provided further evidence that the majority of collagenosomes are distinct from the COPII vesicles and that they primarily represent the sites of type I procollagen biogenesis and not export.

Design of the system for direct visualization of collagenosomes. The structural features of type I collagen biosynthesis can be directly imaged only if full size procollagen polypeptides are used as the fluorescent reporter molecules, because they follow the same modification and folding processes as the endogenous procollagen polypeptides. Therefore, we designed a system for co-expressing fluorescently labeled full size collagen α1(I) and α2(I) polypeptides to directly visualize the collagenosomes. The system consists of three genes, their mRNAs and encoded polypeptides are schematically shown in Fig. 4A. The first gene encodes for full size human collagen α1(I) polypeptide in which we have in frame inserted the sequence of blue fluorescent protein (BFP). By placing the fluorescent tag after the collagen signal peptide sequence, we assured that it will not interfere with the secretion of polypeptide. At this position, the fluorescent tag will also not impede its folding into the triple helix, which starts from the C-terminal end and propagates towards the N-terminus. The mRNA encoding for this α1(I)-BFP fusion reporter (A1-BFP) contained the regulatory 5′ stem-loop (5′SL) sequence, which binds LARP6 and regulates translation. Thus, it visualizes the LARP6 regulated synthesis of α1(I) polypeptide.

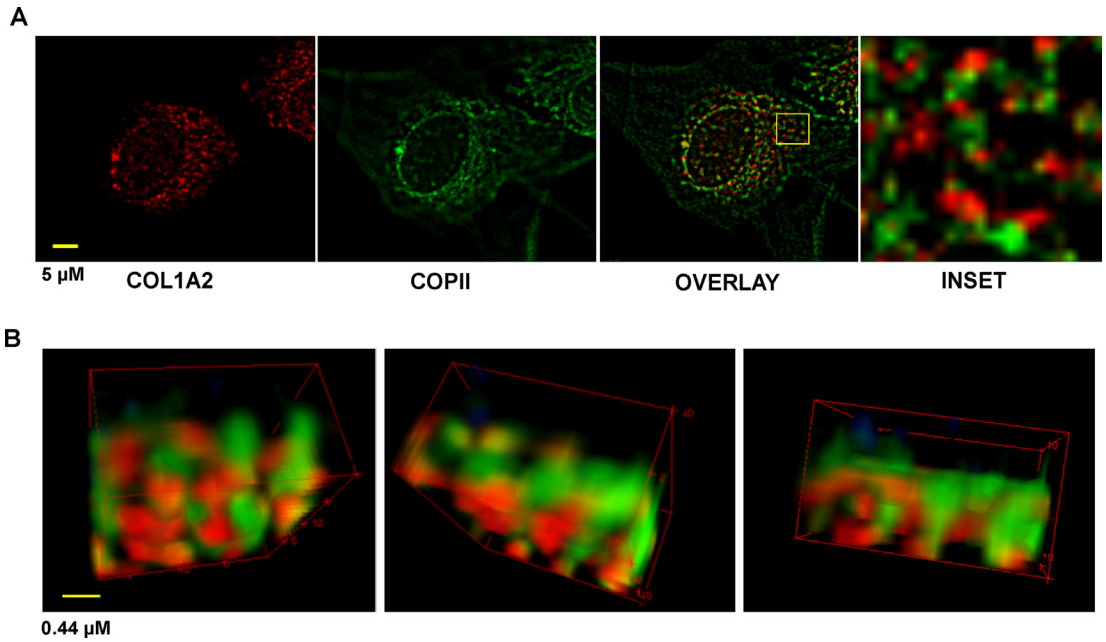

Fig. 3. Collagenosomes and COPII vesicles do not co-localize. Immunostaining of procollagen α2(I) polypeptide (red), COPII protein (green) and overlay of the images. Inset: enlargement of the squared area of the overlay image, (Keyence BZ-X710). B. 3D image of collagenosomes (red) and COPII (green) in co-immunostained HLF. Three different angles of view of the same group of vesicles is shown. The image was reconstructed from 11 confocal images, (OMX Deltavision V4). (For interpretation of the references to color in this figure legend, the reader is referred to the web version of this article.)

The second gene was constructed by placing the sequence of emerald fluorescence protein (GFP) after the signal peptide sequence of the full size human α2(I) cDNA (A2-GFP reporter). The mRNA encoded by this gene also had the 5′SL to report the LARP6 regulated translation of α2(I) polypeptide.

The third gene is similar to the A2-GFP, but the 5′SL was abolished, without changing the coding region (A2Δ5′SL-GFP). Thus, this gene encodes for the identical polypeptide as A2-GFP, but its translation is not regulated by LARP6.

All three reporter genes were driven by the constitutive CMV promoter to report only the differences in posttranscriptional regulation. The reporter genes were transduced into the cells using adenoviruses and co-expression of A1-BFP and A2-GFP or A1-BFP and A2Δ5′SL-GFP in ratio of 2:1 was achieved by transducing the adenoviruses at the relative MOI of 2:1.

Characterization of expression of the reporter genes. To verify the expression of procollagen polypeptides from reporter genes, the genes were first individually transduced into HEK293 cells, which express only tracing amounts of endogenous type I collagen. This allowed assessing the expression of reporters by western blot using both: anti-GFP antibody and anti-collagen antibody (Fig. 4B). Under reducing conditions, in transduced cells the anti-GFP antibody recognized A2-GFP and A2Δ5′SL-GFP fusion polypeptide with apparent molecular weight of 172 kD (left panel, lanes 2 and 3), indicated that full size procollagen α2(I) polypeptide with the GFP tag was expressed. The anti-GFP antibody weakly recognized A1-BFP polypeptide, presumably because it weakly cross-reacted with the BFP tag (lane 1). Nontransduced cells showed no signal with anti-GFP antibody (lane 4).

For confirmation, we re-analyzed the samples using anti-collagen antibody (Fig. 4B, right panel). This antibody recognized A1-BFP, A2-GFP and A2Δ5′SL-GFP polypeptides in the transduced cells, while control cells showed only weak signal of the endogenous protein. These experiments verified that the tagged, full size collagen polypeptides are expressed from our reporter genes.

To verify that A2-GFP co-expressed with A1-BFP folds into disulfide bonded, high molecular weight trimer, indicative of formation of the triple helix of type I procollagen, we co-expressed A1-BFP and A2-GFP or A1-BFP and A2Δ5′SL-GFP at MOI of 2:1 in HLFs. Then, we prepared whole cell extract or purified microsomes from these cells, and analyzed the extract and microsomes using anti-GFP antibody and western blots under non-reducing conditions. If a trimer of two A1-BFP and one A2-GFP polypeptides is formed, it would be recognized by anti-GFP antibody as a disulfide bonded complex of ~ 500 kD. As shown if Fig 4C, a high molecular weight complex was detected in

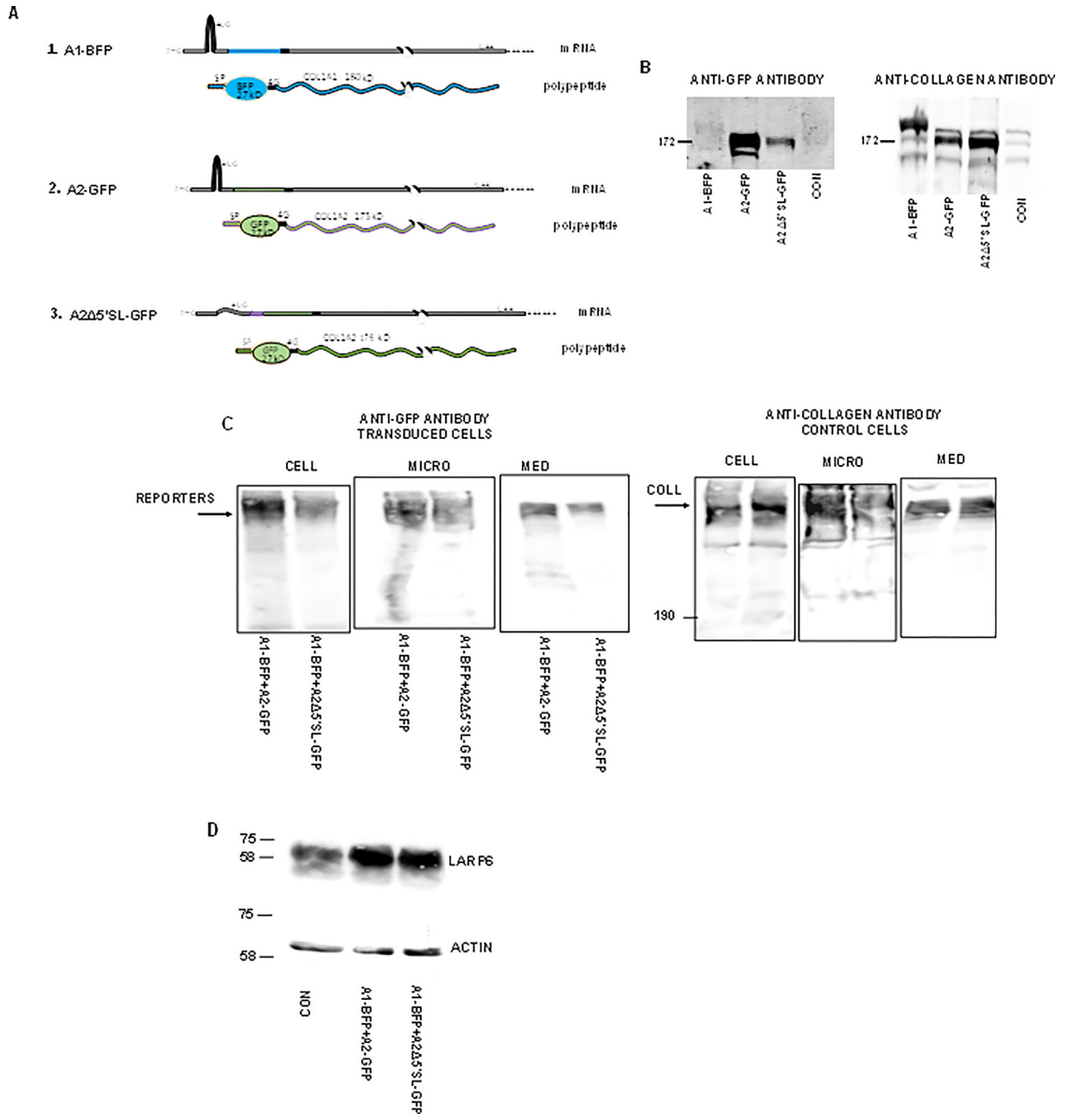

Fig. 4. Design of fluorescently labeled full size type I procollagen reporter polypeptides. A. Schematic representation of the constructs. mRNA is shown as straight line and polypeptide as wavy line. B. Expression of individual reporter polypeptides. Western blot of HEK293 cells transduced with the indicated reporters. Left panel was probed with anti-GFP antibody and right panel with anti-collagen antibody. CON, nontransduced cells. C. Western blot under nonreducing conditions. Left panels: HLFs were transduced with the indicated reporters, total cell extract (CELL), purified microsomes (MICRO) and cellular medium (MED) were analyzed on 4% SDS-PAGE under nonreducing conditions. The samples were run on the same gel and blot probed with anti-GFP antibody. Right panel: control, nontransduced cells were analyzed using anti-collagen antibody in duplicate. D. Expression of LARP6. Western blot of LARP6 in nontransduced HLFs (CON) and in HLFs expressing the indicated reporters. Loading control: actin (ACT).

both, the whole cell extract (left panel, lanes 1 and 2), and in microsomes (lanes 3 and 4). This complex was of high molecular weight and much larger than the single A2-GFP polypeptide, indicating the formation of the disulfide bonded trimer. The trimer was also secreted into the cellular medium (left panel, lanes 5 and 6). The electrophoretic migration of the trimer formed by

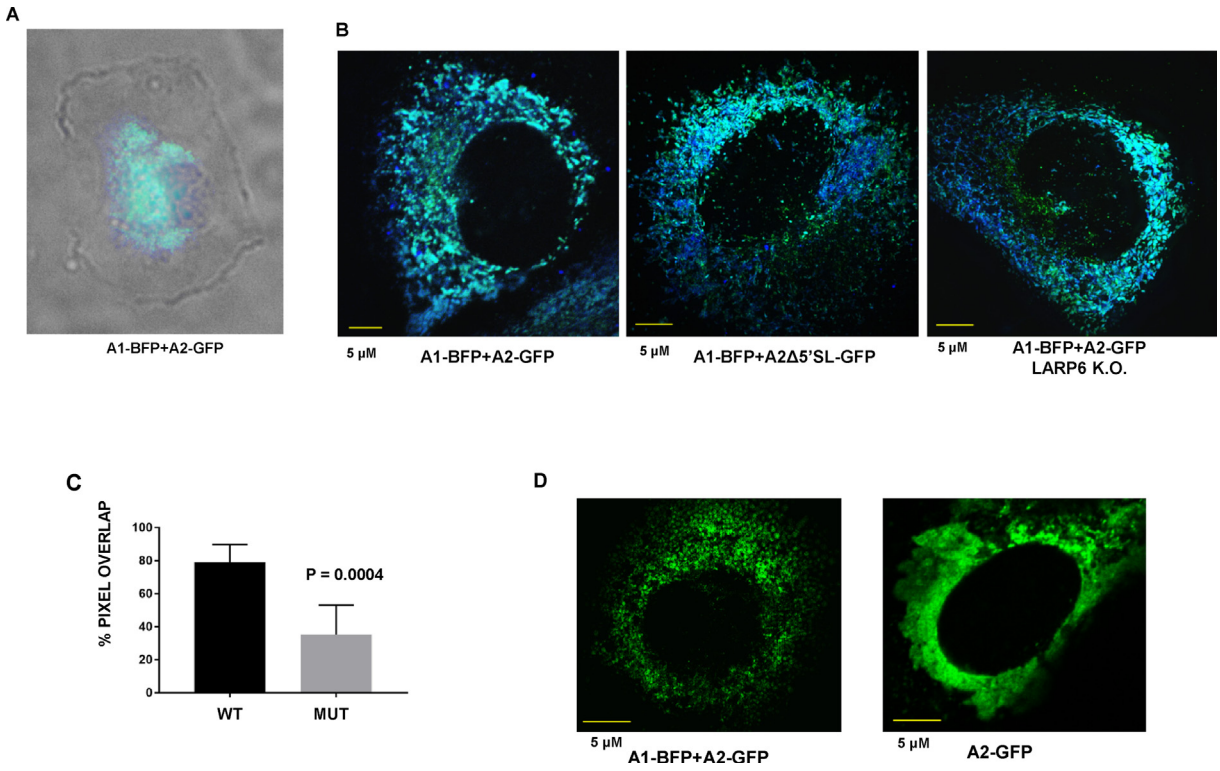

Fig. 5. Imaging of fluorescent collagenosomes. A. Perinuclear localization of fluorescent collagenosomes. Overlay of phase contrast image and fluorescent image of HLF expressing A1-BFP + A2-GFP reporters, (Evos FL). B. High resolution image of collagenosomes in HLFs. Wt HLF was transduced with A1-BFP + A2-GFP (left panel) or A1-BFP + A2-Δ5′SLGFP (middle panel) reporters and LARP6 K.O. HLF was transduced with A1-BFP + A2-GFP reporter (right panel). Confocal images of fixed cells with overlayed blue and green fluorescence are shown, (OMX Deltavision V4). C. Quantification of fluorescence colocalization. Cyan pixels and green pixels were counted from multiple areas of six HLFs transduced with the indicated reporters and number of cyan pixels was normalized to number of green pixels and shown as percent pixel overlap. Error bars: +- 1SD. D. Green fluorescence image of a cell expressing A1-BFP + A2-GFP reporters (left panel) and a cell expressing only A2-GFP reporter, (OMX Deltavision V4). (For interpretation of the references to color in this figure legend, the reader is referred to the web version of this article.)

the reporter polypeptides was similar to that of endogenous type I procollagen trimer, which we analyzed on a parallel gel (Fig. 4C, right panel).

From these experiments we concluded that the polypeptides from the reporter genes assemble into disulfide bonded high molecular weight procollagen with similar electrophoretic mobility as the endogenous type I procollagen, the reporter procollagen co-purifies with the microsomal membranes and is secreted out of the cells. Therefore, we concluded that placing the fluorescent tags does not impede proper formation of type I procollagen.

Expression of reporter genes upregulates endogenous LARP6. LARP6 is required for regulation of translation of type I collagen mRNAs [32,49]. So, the pertinent question was whether the amount of endogenous LARP6 is sufficient to regulate the increased load of collagen mRNAs when the reporter genes are introduced into cells or whether the transduced cells have to be supplemented with exogenous LARP6? Thus, we analyzed the level of endogenous LARP6 in control HLFs and in HLFs expressing A1-BFP + A2-GFP or A1-BFP + A2Δ5′SL-GFP (Fig. 4D). The expression of LARP6 was upregulated when the reporter mRNAs were introduced into the cells, suggesting that the cells compensate for the increased burden of collagen mRNAs by upregulating LARP6. We also supplemented LARP6 to these cells, but did not see any difference in the formation of collagenosomes. This suggested that there is a feedback between the burden of collagen mRNAs and LARP6 expression and that our system does not require LARP6 supplementation.

Perinuclear localization of collagenosomes visualized by fluorescent imaging of reporter polypeptides. To visualize fluorescent collagenosomes we transduced HLFs with A1-BFP + A2-GFP reporters in ratio 2:1 and allowed for 2 days for expression and equilibration to the steady state. Then, we imaged the cells with phase contrast and with blue and green fluorescence and overlaid the images. The

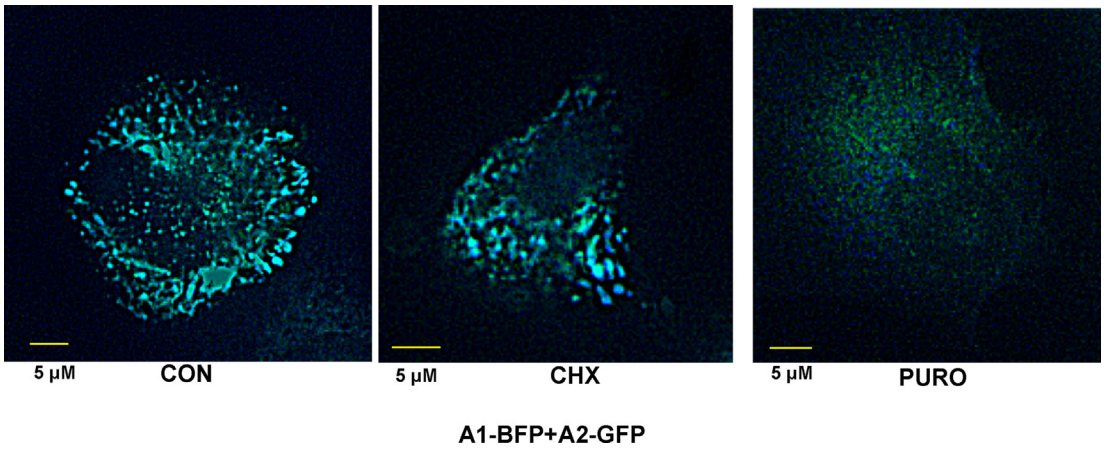

Fig. 6. Intact polysomes are required for collagenosomes formation. HLFs transduced with A1-BFP + A2-GFP reporters were left untreated (CON, left panel) or were treated for 30 min with cycloheximide (CHX, middle panel) or puromycin (PUR, right panel), (Keyence BZ-X710).

fluorescent signals mostly overlapped and were confined to the perinuclear space, without spreading to the periphery of cells (Fig. 5A). The perinuclear localization is consistent with their confinement to the ER, what was suggested before by their presence in the microsomal fraction (Fig. 2C). Therefore, in the subsequent images we show only the fluorescent signal, with the stipulation that the actual cell size is larger than the fluorescent image shown.

High resolution images of collagenosomes in HLFs. To image collagenosomes at high resolution we co-expressed A1-BFP + A2-GFP or A1-BFP + A2Δ5′SL-GFP in HLFs, fixed the cells and took high resolution confocal images with Deltavision OMX V4 microscope. Fig. 5B, left panel, shows the overlaid image of blue fluorescence, displaying the α1(I) polypeptide, and green fluorescence, displaying the α2(I) polypeptide when its expression is LARP6 regulated (A1-BFP + A2-GFP). Many discrete foci, either single or coalesced, of overlapped blue and green fluorescence (cyan color) were seen in the perinuclear space. Small number of foci showed only blue fluorescence or green fluorescence, suggesting that in some foci only the individual polypeptides had accumulated. However, in the majority of collagenosomes there was an overlap of blue and green fluorescence, indicating that these are the sites of folding of α1(I) and α2(I) polypeptides into the procollagen.

The middle panel of Fig. 5B shows the collagenosomes when α2(I) polypeptide is encoded by the mRNA without 5′SL (A1-BFP + A2 Δ5′SL-GFP). The degree of colocalization of α1(I) and α2(I) polypeptides was reduced, the foci showing only the blue or only green fluorescence were more numerous and the collagenosomes appeared more dispersed. Type I procollagen could still be formed, because ~ 30% of collagenosomes showed the cyan color, but the process appeared inefficient and poorly coordinated.

Fig. 5B, right panel shows the collagenosomes in a LARP6 knock out HLF after expression of the A1-BFP + A2-GFP reporters. The collagenosomes looked similar to those seen for A1-BFP + A2Δ5′S L-GFP reporter in wt cells (middle panel), indicating that mutation of 5′SL or knock down of LARP6 give similar phenotypes. The image of collagenosomes in a LARP6 knock out cell of different clonal origin is shown in supplemental Fig. 4. The fact that abolishing the LARP6 binding site or knock down of LARP6 result in similar phenotypes, strongly suggests that binding of LARP6 regulates formation of collagenosomes.

To quantify the colocalization of α1(I) and α2(I) polypeptides when expressed from A1-BFP + A2-GFP reporters and A1-BFP + A2Δ5′SL-GFP reporters, we obtained images of six HLFs expressing the reporters and counted pixels from ~ 3000 collagenosomes. The number of cyan pixels (colocalization of α1(I) and α2(I) polypeptides) was normalized to the number of green pixels (total α2(I) polypeptide) and plotted as the percent of pixel overlap (Fig. 5C). For the A1-BFP + A2-GFP, 79% of green pixels overlapped with blue pixels, while for the A1-BFP + A2Δ5′SL-GFP the overlap was only 35%. This implicates that when collagen α2(I) polypeptide is encoded without LARP6 regulation, type I collagen biogenesis is reduced by ~ 50%. Thus, these experiments verified the observation that binding of LARP6 is not absolutely necessary for type I collagen expression [51], but that it augments the biosynthesis in fibrosis [27].

Formation of collagenosomes is dependent on presence of both procollagen polypeptides. The trimerization of α2(I) polypeptides in the absence of α1(I) polypeptides has never been observed

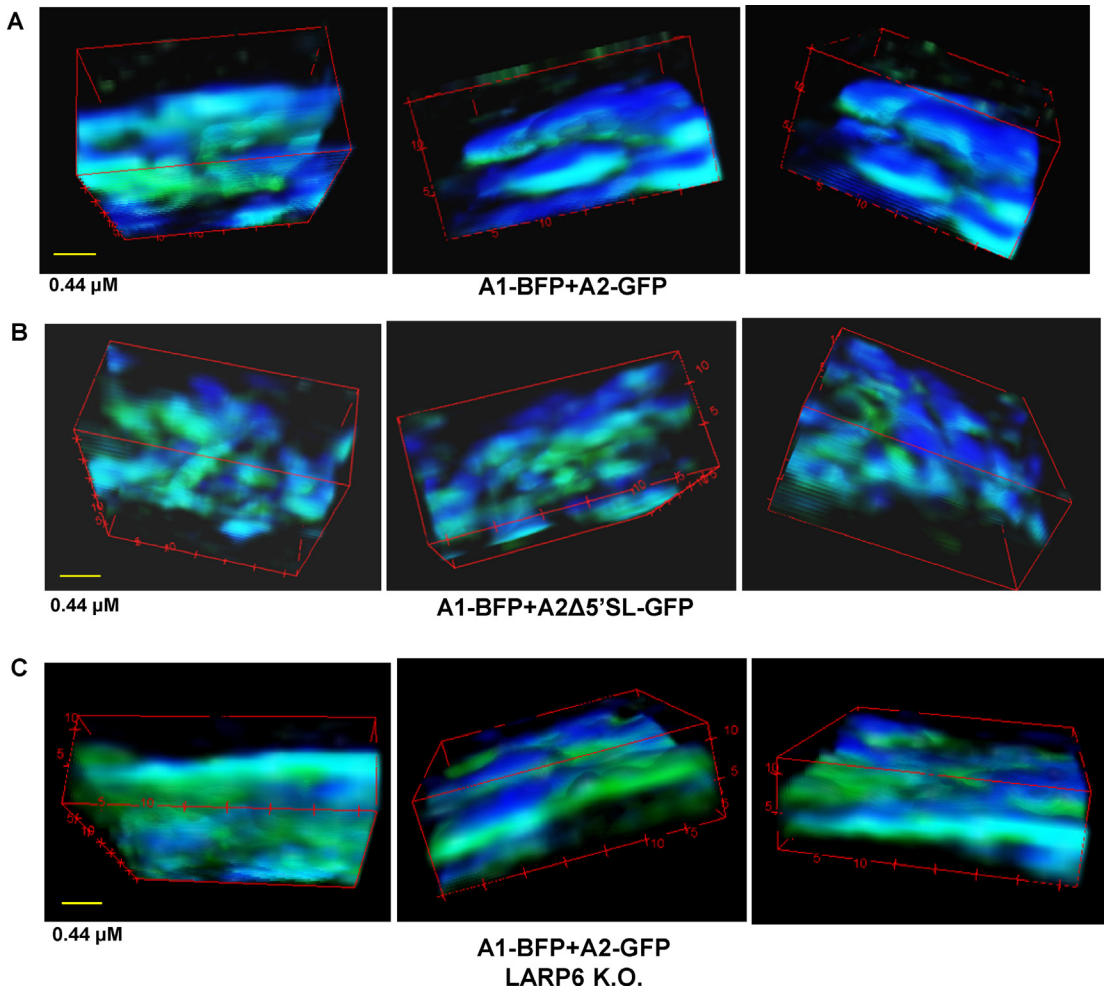

Fig. 7. Collagenosomes as discrete bodies of type I collagen biogenesis. A. 3D image of collagenosomes in A1-BFP + A2-GFP transduced wt HLFs, obtained from 13 confocal images of 0.125 μM arranged in a stack. Different angles of view of the same group of collagenosomes is shown, (OMX Deltavision V4). B. 3D image of collagenosomes in A1-BFP + A2-Δ5′SLGFP transduced wt HLFs. The image was reconstructed from 14 confocal images. C. 3D image of collagenosomes in A1-BFP + A2-GFP transduced LARP6 K.O. HLFs. The image was reconstructed from 11 confocal images, (OMX Deltavision V4.

[52]. Therefore, we tested if collagenosomes can be formed if α2(I) polypeptide is expressed without α1 (I) polypeptide. We transduced HLFs with A1-BFP + A2-GFP or with A2-GFP alone, fixed the cells and imaged the green fluorescence. Fig. 5D shows that collagenosomes were formed when α1(I) polypeptide was co-expressed (left panel), while they were mostly absent when α2(I) polypeptide was expressed alone (right panel). This further confirmed that our system faithfully displays the intricacies of type I collagen biogenesis.

Formation of fluorescent collagenosomes is dependent on the integrity of polysomes. To verify that intact polysomes must be present for the formation of fluorescent collagenosomes, as was demonstrated for the endogenous collagenosomes (Fig. 1), we expressed A1-BFP + A2-GFP reporters in HLFs and treated the cells with cycloheximide and puromycin (Fig. 6). When polysomes were preserved by cycloheximide, the collagenosomes retained their structure (Fig. 6, middle panel). However, when polysomes were dissociated, collagenosomes disappeared (Fig. 6, right panel). Thus, the formation of collagenosomes from the reporter polypeptides is dependent on the integrity of polysomes and recapitulates the requirement for the assembled translational machinery for their existence.

Dissociation of polysomes by puromycin is reversible and when puromycin is removed, the cells reassemble the polysomes. Supplemental Fig. 5 shows that the disruption of collagenosomes by puromycin was also reversible, because when the puromycin was washed off the collagenosomes reformed within 1 h.

Ascorbic acid is a cofactor of prolyl hydroxylases and it has been shown that it stimulates procollagen

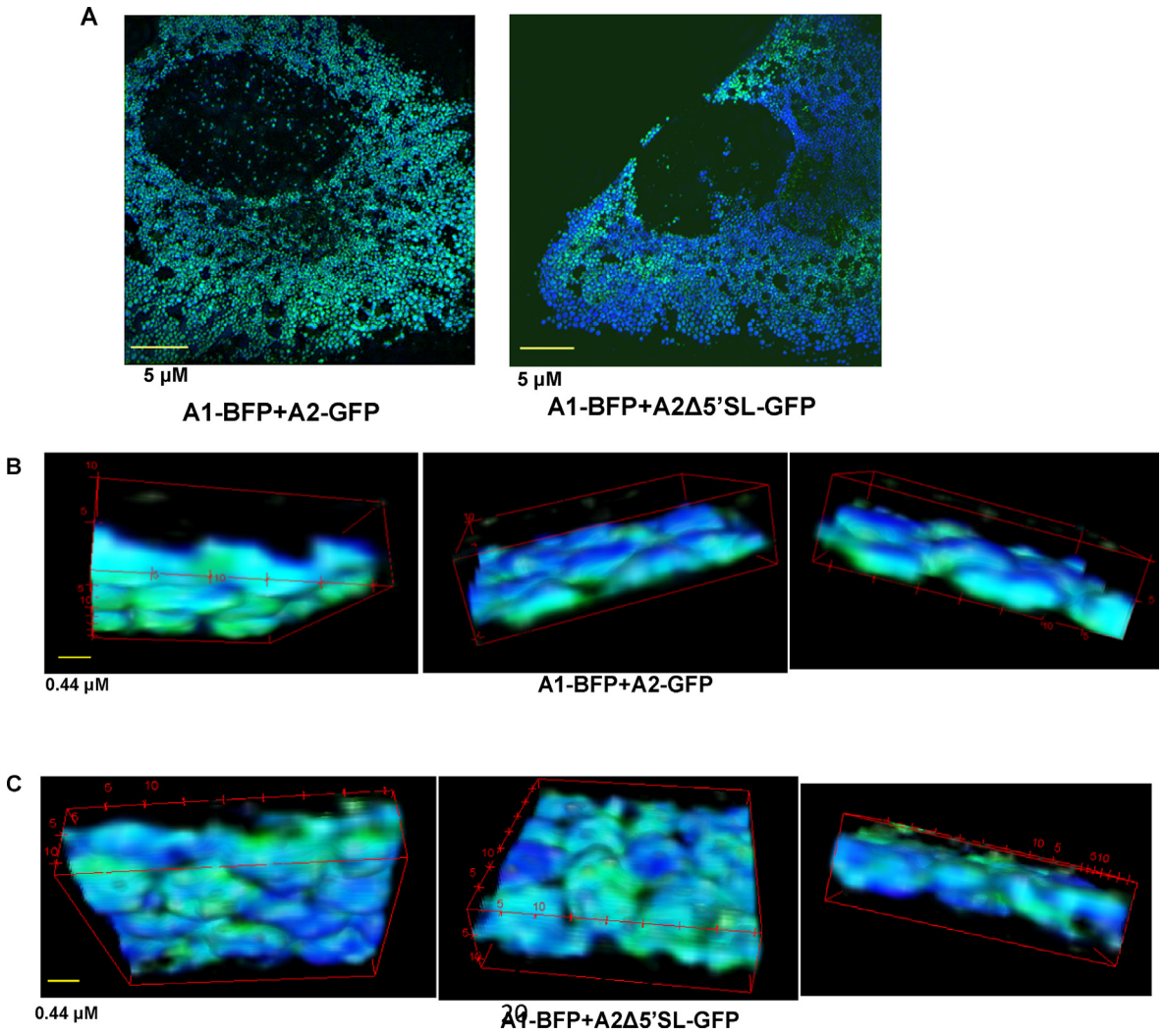

Fig. 8. Collagenosomes in HSCs. A. Image of collagenosomes in HSCs. HSCs were transduced with A1-BFP + A2-GFP (left panel) or A1-BFP + A2-Δ5′SLGFP (right panel) reporters. Confocal image of overlayed blue and green fluorescence was obtained after fixing the cells, (OMX Deltavision V4). B. 3D image of collagenosomes in A1-BFP + A2-GFP transduced HSCs, obtained from 12 confocal images of 0.125 μM arranged in a stack. Different angles of view of the same group of collagenosomes is shown, (OMX Deltavision V4). C. 3D image of collagenosomes in A1-BFP + A2-Δ5′SLGFP transduced wt HSCs. The image was reconstructed from 12 confocal images, (OMX Deltavision V4). (For interpretation of the references to color in this figure legend, the reader is referred to the web version of this article.)

secretion from osteoblasts [53]. Therefore, we tested if the treatment of HLFs with ascorbic acid would alter the appearance of collagenosomes. Supplemental Fig. 6 shows that in HLFs ascorbic acid did not change the general appearance of collagenosomes, suggesting that facilitating prolyl hydroxylation has no effect on the collagenosomes in HLFs.

Collagenosomes are highly organized bodies of type I procollagen biogenesis. To obtain 3D images of collagenosomes we took 11–13 high resolution confocal slices of HLFs, arranged them in a Z-stack and reconstructed 3D images. Fig. 7A shows three different angles of collagenosomes formed by A1-BFP + A2-GFP reporter polypeptides. These collagenosomes were disk shaped bodies with diameter of 0.5–1 μM and thickness of 200–400 nM. The fluorescent collagenosomes appeared more uniform in size and shape than the collagenosomes revealed by immunostaining (Fig. 1D), presumably because the direct visualization was devoid of the artifacts of using fluorescent antibodies. Nevertheless, the fluorescent collagenosomes resembled the disk shape of the endogenous collagenosomes, suggesting that they are not an artifact of the expression of reporter genes. Interestingly, on the top of collagenosomes the A1BFP signal was predominant, while on the bottom the A2GFP signal was predominant. However, in the body of

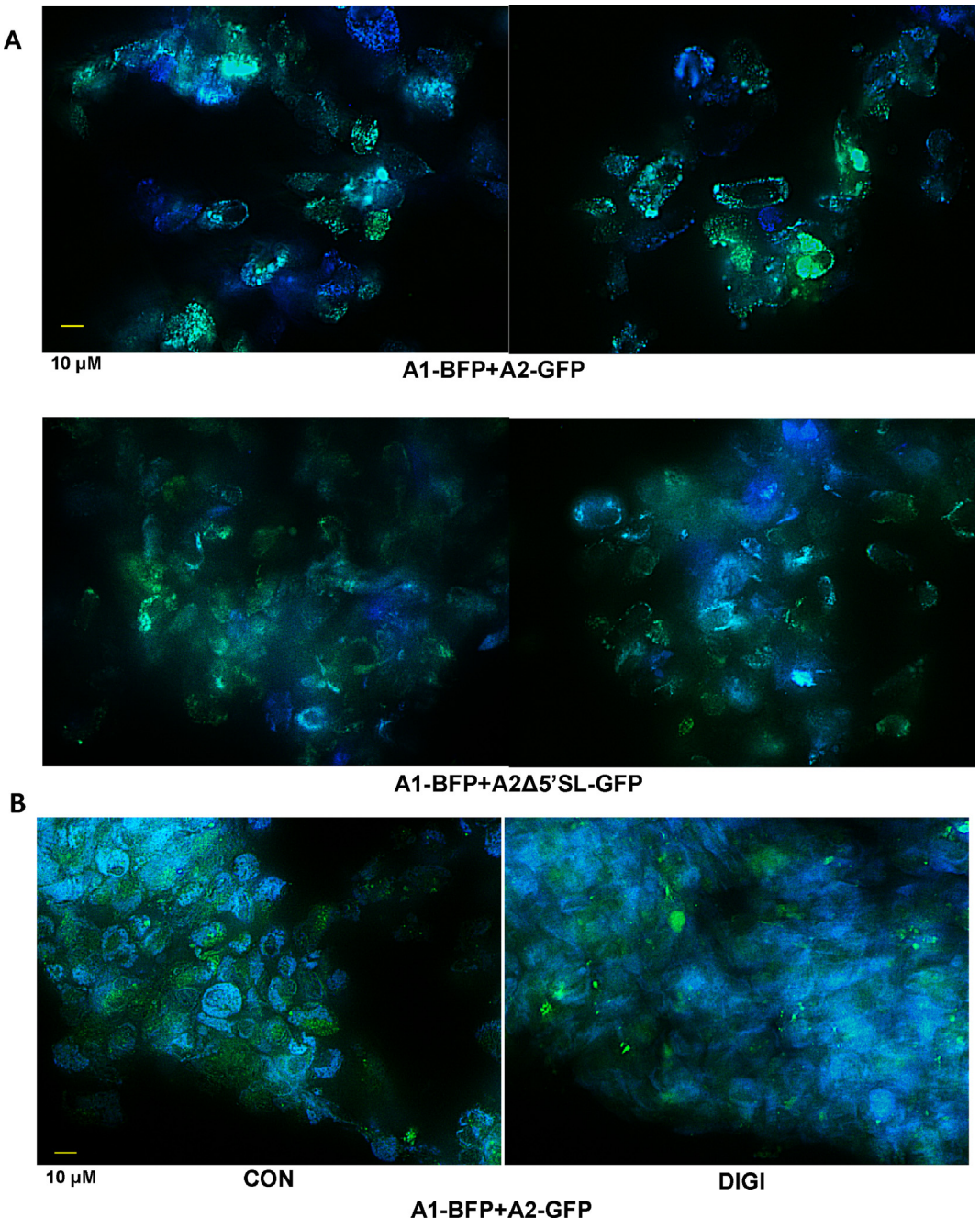

Fig. 9. Fluorescent collagenosomes purify with microsomal membranes. A. Image of fluorescence of microsomes in HLFs. Two confocal images of microsomes purified from HLFs expressing A1-BFP + A2-GFP reporters (upper panels) and from HLFs expressing A1-BFP + A2-Δ5′SLGFP reporters. Overlay of blue and green fluorescence is shown, (Keyence BZ-X710). B. Dispersion of microsomal membranes by detergent releases collagenosomes. Microsomal membranes were untreated (CON) or treated with digitonin (DIGI) before taking the images, (Keyence BZ-X710). (For interpretation of the references to color in this figure legend, the reader is referred to the web version of this article.)

the particles there was the overlap of green and blue fluorescence (cyan color), indicating the colocalization of the polypeptides and that the folding of procollagen trimer takes place inside the particle.

The three images in Fig. 7B show the collagenosomes which form when α2(I) polypeptide is translated without LARP6 regulation, what was achieved by expressing A1-BFP + A2Δ5′SL-GFP reporter genes. These

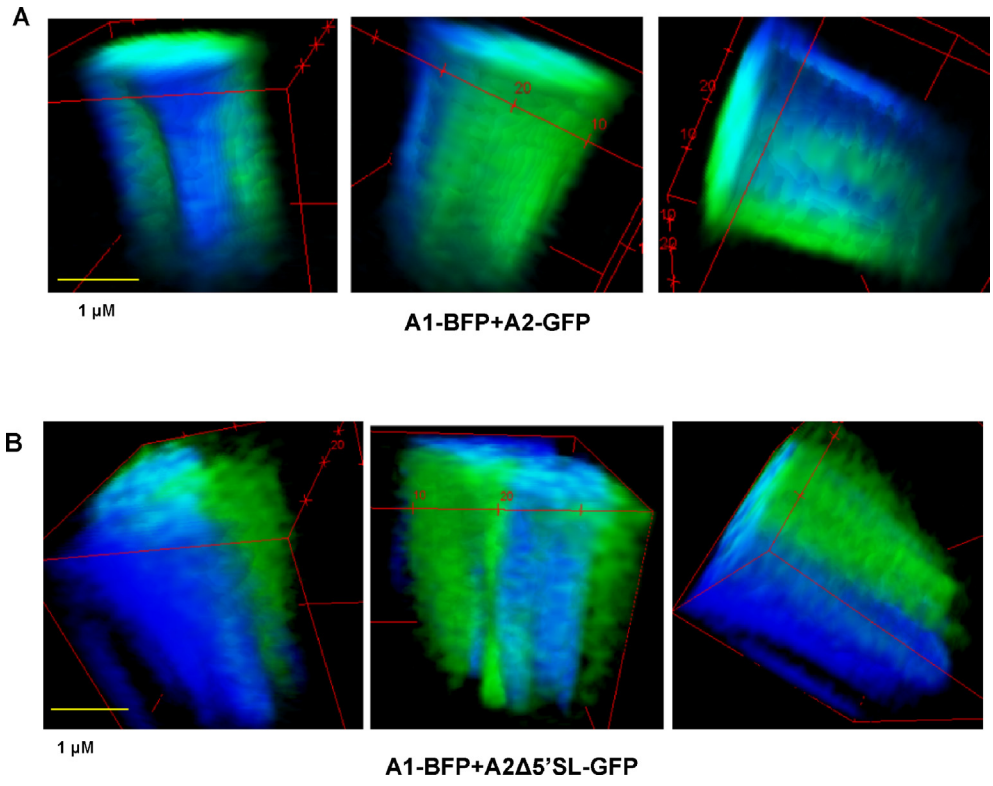

Fig. 10. 3D image of fluorescent collagenosomes in microsomal membrane. A. Three different angles of view of a 3x zoomed image of A1-BFP + A2-GFP collagenosomes reconstructed from 40 confocal images of 0.1 μM. B. A1-BFP + A2-Δ5′SLGFP collagenosomes reconstructed from 41 confocal images, (Keyence BZ-X710).

collagenosomes were also resolved as discrete bodies, but they were smaller, irregular in shape and the overlap of A1-BFP and A2-GFP in the body of the particles was diminished. The segregation of the A1-BFP on the top of the collagenosomes and A2-GFP on the bottom was also not so distinctly preserved.

We also reconstructed the 3D collagenosomes in LARP6 knock out cells by expressing A1-BFP + A2-GFP reporters (Fig. 7C). Although both of these reporter genes contained the 5′SL, without LARP6 in the cells the collagenosomes had irregular shape and diminished overlap of the α1(I) and α2 (I) polypeptides in the body of the particles. This suggested that the shape and size of collagenosomes and the folding of collagen polypeptides in their interior are the processes regulated by LARP6 binding to the 5′SL of collagen mRNAs.

Collagenosomes have similar structure in other collagen producing cells. Activated hepatic stellate cells (HSCs) are liver myofobroblasts responsible for type I collagen production in hepatic fibrosis. We reconstructed the 3D image of collagenosomes in HSCs for comparison to HLFs. Fig. 8A shows one confocal plane of a HSC expressing A1-BFP + A2-GFP reporters (left panel) and A1-BFP + A2Δ5′SL-GFP reporters (right panel). Numerous, collagenosomes with a high degree of overlap of blue and green fluorescence was seen with the A1-BFP + A2-GFP reporters, while the colocalization of blue and green fluorescence in the most collagenosomes of A1-BFP + A2Δ5′SL-GFP reporters was diminished. When the 3D images of collagenosomes were reconstructed, the A1-BFP + A2-GFP collagenosomes were similar in size to that in HLFs, with overlapping α1(I) and α2 (I) polypeptides in the interior of particles (Fig. 8B). Again, the predominant location of the individual α1(I) polypeptides was on the top of collagenosomes, while the individual α2(I) polypeptides was at the bottom. Thus, this particular organization of type I collagen biogenesis seems to be a general feature of collagen producing cells.

In contrast, the A1-BFP + A2Δ5′SL-GFP collagenosomes were poorly organized with diminished overlap of blue and green fluorescence in the core of particles and lack of clear segregation of individual polypeptides to the opposite sides of particles (Fig. 8C). These images clearly demonstrated that folding of type I procollagen in hepatic stellate cells takes place in highly organized structures, collagenosomes, formation of which critically depends on the LARP6 regulated translation of collagen mRNAs.

Fluorescent collagenosomes are associated with the ER membrane. Because the endogenous collagenosomes fractionated with the ER membrane (Fig. 2), we analyzed if the fluorescent collagenosomes will show the same partitioning. Therefore, we isolated microsomes from cells expressing A1-BFP + A2-GFP or A1-BFP + A2Δ5′ SL-GFP reporters and imaged the fluorescence of microsomes. Fig. 9A, top panels, shows the A1-BFP + A2-GFP collagenosomes in microsomal membranes. The granular pattern is clearly discernable, but the collagenosomes were not as distinctly organized as in intact cells, probably due to disruption and re-assembly of the ER membranes during the isolation procedure [54]. The A1-BFP + A2Δ5′SL-GFP collagenosomes could not be discerned as individual particles and the fluorescent signals appeared diffuse (Fig. 9A, lower panels).

Digitonin is detergent commonly used to solubilize ER membranes [55,56]. When the isolated microsomal membranes were treated with digitonin, the granular pattern of collagenosomes seen in intact membranes (Fig. 9B, right panel), disappeared and fluorescence became diffused (Fig. 9B, lower panel), further confirming their intimate association with the ER membranes.

3D images of fluorescent collagenosomes in microsomal membranes. To assess if the fluorescent collagenosomes show cylindrical structures in the microsomal membranes as the endogenous collagenosomes (Fig. 2E) we reconstructed the confocal images of A1-BFP + A2-GFP or A1-BFP + A2Δ5′SL-GFP collagenosomes into stacks. The cylindrical structures were revealed, which for A1-BFP + A2-GFP reporters showed a large central core with the overlap of blue and green fluorescence, while the individual polypeptides were partitioned to the outer edges of the cylinders (Fig. 10A). The colocalization of α1(I) and α2(I) polypeptides in the core and the segregation of individual polypeptides to the periphery was similar to that in collagenosomes in intact cells, except the cylinders may have formed by coalescence of individual collagenosomes into larger assemblies upon reassembly of the microsomes. The finding that procollagen α1(I) and α2(I) polypeptides colocalize while they are still associated with the ER membrane strongly suggests that the biogenesis of type I procollagen is membrane associated.

The A1-BFP + A2Δ5′SL-GFP collagenosome cylinders showed diminished fluorescence overlap in the core (Fig. 10B), indicating that they are poorly organized.

Collagenosomes are stable structures in live cells. To image the dynamics of collagenosomes in cells we obtained confocal images of live cells expressing A1-BFP + A2-GFP reporters at 30-min intervals. Supplemental Fig. 7 shows that collagenosomes change very little during the 3.5 h period, suggesting that they are relatively stable structures. Time points longer than several hours showed changes caused by migration of cells, but we have not observed dramatic alteration in the general appearance of collagenosomes within 24 h.

Discussion

Tagging of type I collagen polypeptides with fluorescence tags has been published before [18,57]. Lu et al. tagged α2(I) polypeptide and followed its assembly into procollagen in osteoblasts and the role of fibronectin in this process. The authors focused on imaging of fibril networks and collagen bundles and on dynamics of these structures secreted by live cells [57]. On the contrary, in this work we focused on the high-resolution imaging of the early events in the procollagen biosynthetic pathway that take place on the ER membrane. We used cells responsible for pulmonary, dermal and hepatic fibrosis and visualized the assembly of the type I procollagen heterotrimers by simultaneously tagging both polypeptides. In this way we were able to demonstrate type I procollagen biosynthesis in highly organized bodies associated with the ER membrane.

Type I collagen biosynthesis is complex, involving translation, posttranslational modifications and registration of two α1(I) polypeptides and one α2(I) polypeptide to initiate folding into the triple helix [2]. It takes about 18 min from the initiation of translation of type I collagen mRNAs to the appearance of folded type I procollagen in the cellular medium [58]. The translation elongation takes about 5 min to yield a full-size procollagen polypeptide, assuming the translational rate of 330 codons/min [59]. In chicken tendon fibroblasts it takes 8.5 min for 50% of the type I collagen molecules to fold into triple helix [4]. During this time the isomerization of Gly-Pro bonds in nascent polypeptides, their posttranslational modifications, the registration of three polypeptides at the C-terminus and their folding into triple helix must be accomplished. The two slowest steps in this pathway are formation of C-terminally nucleated trimer to initiate the folding [52,60] and cis–trans isomerization of Gly-Pro bonds [8,61]. The peptidyl-prolyl cis–*trans*-isomerase is ER membrane bound [62], so cis–*trans*-isomerization can commence during the translational elongation. It has also been reported that procollagen polypeptides can fold into triple helix while still associated with polysomes on the ER membrane [63], what would accelerate the process. Our results support this finding.

After folding, the helices are exported out of the ER by the TANGO1 coated COPI II vesicles [50,64] and secreted out of the cells; 4.5 min are left for this process. COPI II vesicles also form on the ER membrane [65], thus, procollagen polypeptides

are retained on the ER membrane for prolonged periods of time during the biogenesis of type I procollagen. Therefore, it is not surprising that we found intracellular type I procollagen predominantly associated with the microsomal membranes and demonstrated colocalization of two type I collagen polypeptides on these membranes (Figs. 2, 4, 9 and 10).

The new finding of this work is that type I procollagen polypeptides are not randomly and diffusely translated on the ER membrane, but they are made in highly organized bodies which we termed the collagenosomes. The formation of collagenosomes was demonstrated in cultured fibroblasts and hepatic stellate cells, which produce large amounts of type I procollagen in vitro. Whether collagenosomes form when these cells are in quiescent state and maintain only the low rate biosynthesis, remains to be determined. When the endogenous type I procollagen is immunostained in cultured cells, a focal pattern of localization within the ER is apparent and seen in several types of collagen producing cells (Fig. 1). The existence of these foci is dependent on the integrity of polysomes (Figs. 1 and 6), suggesting that they represent nascent sites of biogenesis, rather than the TANGO1 organized COPI II export vesicles. This is also supported by our findings that most collagenosomes do not colocalize with the COPII containing vesicles and that they are spatially segregated (Fig. 3). However, a small number of collagenosomes and COPII vesicles appear to have a partial overlap. This may simply be due to the molecular crowding on the ER membrane or it may suggest that there is some extent of coupling of the biosynthesis and export. Therefore, the functional significance of this finding remains to be explored.

To facilitate studying type I collagen biogenesis we constructed a reporter system in which full size α1(I) and α2(I) polypeptides are tagged with different fluorescence tags to allow their direct visualization (Fig. 4A). The fluorescent tags were placed after the signal peptide sequence, so they are retained after the insertion of reporter polypeptides into the ER and do not interfere with registration and folding into triple helix (Fig. 4C) [52,60]. In this way the reporters faithfully mimic the endogenous polypeptides with respect to the size of triple helical region, posttranslational modifications, foldability and export. The system also allowed assessment of the role of LARP6 in these processes, because the identical α2(I) polypeptides can be made by the mRNA with or without 5′ SL. To facilitate the analysis 5′SL mutation was made in the context of α2(I) mRNA, because α2(I) polypeptides cannot self-associate into homotrimers. We clearly demonstrated that collagenosomes do not form if A2-GFP reporter is expressed alone (Fig. 5D).

One important finding using our system was that the expression of endogenous LARP6 was upregulated when the reporters were introduced into the cells (Fig. 4D). This suggests that there is a crosstalk between the level of collagen mRNAs present in the cell and expression of LARP6. The nature of this feedback mechanism is not known, but is important to elucidate, because it may be a fundamental mechanism that allows increased type I collagen production in fibrosis.

High resolution images of collagenosomes in cells revealed that they are discrete bodies (Figs. 7 and 8). Individual collagenosomes appear as disks with diameter of 0.5–1 μM and thickness of 200–400 nM, with colocalization of α1(I) and α2(I) polypeptides in the core of particle. A single triple helix of type I collagen has a length of 300 nM and width of 1.5 nM. This suggests that many collagen helices can be accommodated within the core of collagenosomes if they are laterally positioned. The non-colocalized polypeptides were segregated on the opposite peripheries of the disks. One possibility is that the individual polypeptides are fed into the folding core from the opposite sides to help the lateral positioning of folded molecules. Alternatively, they may be extruded from the core to the opposite sides if they are not assembled into the triple helix. Our display of collagenosomes in actively collagen producing cells indicates that the biogenesis of type I procollagen is highly organized process associated with the ER membrane. The mechanistic details of this process will be elucidated upon resolving the structure of collagenosomes by cryo-EM.

LARP6 is the protein which regulates translation of type I collagen mRNAs [31–33]. Because formation of collagenosomes is dependent on integrity of translational machinery (Fig. 1A and 6), the role of LARP6 in organizing collagenosomes is not surprising. We have demonstrated such role by two approaches; knocking down of LARP6 and mutation of its binding site in collagen α2(I) mRNA result in poor organization of collagenosomes and 50% reduced colocalization of α1(I) and α2(I) polypeptides. This confirms the previous observations that the LARP6 regulation is not absolutely necessary for type I collagen production, but that it accelerates the biosynthesis in fibrosis [27].

Collagenosomes copurify with microsomal membranes (Figs. 2 and 9), while dissolving the membranes with detergent causes their dispersion, suggesting that their organization depends on the ER membrane integrity. In purified membranes collagenosomes appeared coalesced in cylinders (Figs. 2 and 10), what may be an artifact of cell homogenization and re-assembly of internal membranes during the purification process. Nevertheless, the folding of α1(I) and α2(I) polypeptides was seen in the core of the

cylinders. This finding confirms the previous observation that assembly of type I collagen can take place while the polypeptides are still associated with the ER membrane [63].

Collagenosomes appear to be relatively stable structures with little reorganization within several hours. Sequential imaging of live cells shows little changes in the number, size or position of collagenosomes within several hours (supplemental Fig. 7). Thus, once established, collagenosomes can be regarded as stable assemblies of type I collagen biogenesis.

Experiments in vitro with short peptides consisting of GPP repeats have been commonly used to mimic type I procollagen folding [66–68]. They revealed very slow kinetics of folding in vitro. To achieve the rate of folding observed in vivo the peptides had to be in 1 M concentration [12]. Such high concentration of collagen polypeptides is impossible to achieve in the cell and, although in vivo folding is facilitated by molecular chaperones [69], the high concentration dependence of the process suggests that restricting the diffusion of polypeptides in the two dimensions of the ER membrane would accelerate the biogenesis. However, in states of intensive type I collagen production, such as fibrosis, we propose that additional level of organization is needed. This is achieved by formation of collagenosomes, which restrict translation of both type I procollagen polypeptides within a small volume of space, increasing their local concentration to accelerate the processing, nucleation and folding. The concept that complex proteins are synthesized in highly organized structures is not novel. The subunits of proteasome are co-translationally assembled in structures termed “assemblysomes” [63], while ribosome profiling in yeast discovered nine hetero-oligomeric proteins that are co-translationally assembled [64]. It has been postulated that coordination of translation enhances the efficacy of assembly which occurs in synchronization rather than in competition with chaperones [65]. This report extends the concept to type I collagen, but whether the other collagens are also assembled in collagenosomes, remains to be investigated.

With the reporter system described here it will be possible to elucidate the structural and mechanistic aspects of type I collagen biogenesis in collagenosomes, as well as use the system for high throughput screening for LARP6 binding inhibitors as antifibrotic compounds [36,37].

CRediT authorship contribution statement

Branko Stefanovic: Conceptualization, Methodology, Validation, Formal analysis, Investigation, Writing - original draft, Visualization, Supervision, Funding acquisition. **Lela Stefanovic:** Methodology, Investigation. **Zarko Manojlovic:** Methodology, Investigation, Resources, Writing - review & editing.

DECLARATION OF COMPETING INTEREST

The authors declare that they have no known competing financial interests or personal relationships that could have appeared to influence the work reported in this paper.

Acknowledgments

This work has been supported in part by grants from Florida State University Research Foundation to B.S. The authors are indebted to Ruth Didier for assistance with high resolution imaging.

Received 5 February 2021;
Accepted 18 June 2021;
Available online 23 June 2021

Keywords:
Type I collagen;
Biosynthesis;
Imaging in cells;
Colocalization;
Fibrosis

References

1. Chowdhury, S.R., Mh Busra, M.F., Lokanathan, Y., Ng, M. H., Law, J.X., Cletus, U.C., Binti Haji Idrus, R., (2018). Collagen type I: A versatile biomaterial. *Adv. Exp. Med. Biol.*, **1077**, 389–414.
2. Kivirikko, K.I., (1998). Collagen biosynthesis: a mini-review cluster. *Matrix Biol.*, **16** (7), 355–356.
3. Eberhardt, E.S., Panisik Jr., N., Raines, R.T., (1996). Inductive effects on the energetics of prolyl peptide bond isomerization: implications for collagen folding and stability. *J. Am. Chem. Soc.*, **118** (49), 12261–12266.
4. Steinmann, B., Bruckner, P., Superti-Furga, A., (1991). Cyclosporin A slows collagen triple-helix formation in vivo: indirect evidence for a physiologic role of peptidyl-prolyl cis-trans-isomerase. *J. Biol. Chem.*, **266** (2), 1299–1303.
5. Myllyharju, J., (2003). Prolyl 4-hydroxylases, the key enzymes of collagen biosynthesis. *Matrix Biol.*, **22** (1), 15–24.
6. Hennet, T., (2019). Collagen glycosylation. *Curr. Opin. Struct. Biol.*, **56**, 131–138.
7. Scietti, L., Chiapparino, A., De Giorgi, F., Fumagalli, M., Khoriauli, L., Nergadze, S., Basu, S., Olieric, V., Cucca, L., Banushi, B., Profumo, A., Giulotto, E., Gissen, P., Forneris, F., (2018). Molecular architecture of the multifunctional

collagen lysyl hydroxylase and glycosyltransferase LH3. *Nat. Commun.*, **9** (1), 3163.
8. Bachmann, A., Kiefhaber, T., Boudko, S., Engel, J., Bachinger, H.P., (2005). Collagen triple-helix formation in all-trans chains proceeds by a nucleation/growth mechanism with a purely entropic barrier. *Proc. Natl. Acad. Sci. USA*, **102** (39), 13897–13902.
9. Lamande, S.R., Bateman, J.F., (1999). Procollagen folding and assembly: the role of endoplasmic reticulum enzymes and molecular chaperones. *Semin. Cell Dev. Biol.*, **10** (5), 455–464.
10. McLaughlin, S.H., Bulleid, N.J., (1998). Molecular recognition in procollagen chain assembly. *Matrix Biol.*, **16** (7), 369–377.
11. Baum, J., Brodsky, B., (1997). Real-time NMR investigations of triple-helix folding and collagen folding diseases. *Fold Des.*, **2** (4), R53–R60.
12. Boudko, S., Frank, S., Kammerer, R.A., Stetefeld, J., Schulthess, T., Landwehr, R., Lustig, A., Bachinger, H.P., Engel, J., (2002). Nucleation and propagation of the collagen triple helix in single-chain and trimerized peptides: transition from third to first order kinetics. *J. Mol. Biol.*, **317** (3), 459–470.
13. Boudko, S.P., Engel, Jürgen, Bächinger, H.P., (2012). The crucial role of trimerization domains in collagen folding. *Int. J. Biochem. Cell Biol.*, **44** (1), 21–32.
14. Ito, S., Nagata, K., (2019). Roles of the endoplasmic reticulum-resident, collagen-specific molecular chaperone Hsp47 in vertebrate cells and human disease. *J. Biol. Chem.*, **294** (6), 2133–2141.
15. Makareeva, E., Aviles, N.A., Leikin, S., (2011). Chaperoning osteogenesis: new protein-folding disease paradigms. *Trends Cell Biol.*, **21** (3), 168–176.
16. Yuan, L., Kenny, S.J., Hemmati, J., Xu, K., Schekman, R., (2018). TANGO1 and SEC12 are copackaged with procollagen I to facilitate the generation of large COPII carriers. *Proc. Natl. Acad. Sci. USA*, **115** (52), E12255–E12264.
17. Malhotra, V., Erlmann, P., (2015). The pathway of collagen secretion. *Annu. Rev. Cell Dev. Biol.*, **31** (1), 109–124.
18. Omari, S., Makareeva, E., Gorrell, L., Jarnik, M., Lippincott-Schwartz, J., Leikin, S., (2020). Mechanisms of procollagen and HSP47 sorting during ER-to-Golgi trafficking. *Matrix Biol.*, **93**, 79–94.
19. Malfait, F., Symoens, S., Coucke, P., Nunes, L., De Almeida, S., De Paepe, A., (2006). Total absence of the alpha2(I) chain of collagen type I causes a rare form of Ehlers-Danlos syndrome with hypermobility and propensity to cardiac valvular problems. *J. Med. Genet.*, **43**, (7) e36
20. McBride Jr., D.J., Choe, V., Shapiro, J.R., Brodsky, B., (1997). Altered collagen structure in mouse tail tendon lacking the alpha 2(I) chain. *J. Mol. Biol.*, **270** (2), 275–284.
21. Miles, C.A., Sims, T.J., Camacho, N.P., Bailey, A.J., (2002). The role of the alpha2 chain in the stabilization of the collagen type I heterotrimer: a study of the type I homotrimer in oim mouse tissues. *J. Mol. Biol.*, **321** (5), 797–805.
22. Verzijl, N., DeGroot, J., Thorpe, S.R., Bank, R.A., Shaw, J. N., Lyons, T.J., Bijlsma, J.W.J., Lafeber, F.P.J.G., Baynes, J.W., TeKoppele, J.M., (2000). Effect of collagen turnover on the accumulation of advanced glycation end products. *J. Biol. Chem.*, **275** (50), 39027–39031.
23. Sivan, S.-S., Wachtel, E., Tsitron, E., Sakkee, N., van der Ham, F., DeGroot, J., Roberts, S., Maroudas, A., (2008). Collagen turnover in normal and degenerate human intervertebral discs as determined by the racemization of aspartic acid. *J. Biol. Chem.*, **283** (14), 8796–8801.
24. el-Harake, W.A., Furman, M.A., Cook, B., Nair, K.S., Kukowski, J., Brodsky, I.G., (1998). Measurement of dermal collagen synthesis rate in vivo in humans. *Am. J. Physiol.*, **274** (4 Pt 1), E586–E591.
25. Smeets, J.S.J., Horstman, A.M.H., Vles, G.F., Emans, P. J., Goessens, J.P.B., Gijsen, A.P., van Kranenburg, J.M. X., van Loon, L.J.C., (2019). Protein synthesis rates of muscle, tendon, ligament, cartilage, and bone tissue in vivo in humans. *PLoS One*, **14** (11)
26. Decaris, M.L., Emson, C.L., Li, K., Gatmaitan, M., Luo, F., Cattin, J., Nakamura, C., Holmes, W.E., Angel, T.E., Peters, M.G., Turner, S.M., Hellerstein, M.K., Avila, M.A., (2015). Turnover rates of hepatic collagen and circulating collagen-associated proteins in humans with chronic liver disease. *PLoS One*, **10** (4), e0123311.
27. Parsons, C.J., Stefanovic, B., Seki, E., Aoyama, T., Latour, A.M., Marzluff, W.F., Rippe, R.A., Brenner, D.A., (2011). Mutation of the 5' untranslated region stem-loop structure inhibits {alpha}1(i) collagen expression in vivo. *J. Biol. Chem.*, **286** (10), 8609–8619.
28. Zhang, Y., Stefanovic, B., (2016). Akt mediated phosphorylation of LARP6; critical step in biosynthesis of type I collagen. *Sci. Rep.*, **6**, 22597.
29. Zhang, Y., Stefanovic, B., (2016). LARP6 Meets Collagen mRNA: Specific Regulation of Type I Collagen Expression. *Int. J. Mol. Sci.*, **17** (3), 419.
30. Wang, H., Stefanovic, B., Palazzo, A.F., (2014). Role of LARP6 and nonmuscle myosin in partitioning of collagen mRNAs to the ER membrane. *PLoS ONE*, **9** (10), e108870.
31. Stefanovic, L., Longo, L., Zhang, Y., Stefanovic, B., (2014). Characterization of binding of LARP6 to the 5' stem-loop of collagen mRNAs: implications for synthesis of type I collagen. *RNA Biol.*, **11** (11), 1386–1401.
32. Vukmirovic, M., Manojlovic, Z., Stefanovic, B., (2013). Serine-threonine kinase receptor-associated protein (STRAP) regulates translation of type I collagen mRNAs. *Mol. Cell. Biol.*, **33** (19), 3893–3906.
33. Manojlovic, Z., Stefanovic, B., (2012). A novel role of RNA helicase A in regulation of translation of type I collagen mRNAs. *RNA*, **18** (2), 321–334.
34. Challa, A.A., Vukmirovic, M., Blackmon, J., Stefanovic, B., Kocher, O., (2012). Withaferin-A reduces type I collagen expression in vitro and inhibits development of myocardial fibrosis in vivo. *PLoS One*, **7** (8), e42989.
35. Fritz, D., Cai, L., Stefanovic, L., Stefanovic, B., (2011). Progress towards discovery of antifibrotic drugs targeting synthesis of type I collagen. *Curr. Med. Chem.*, **18** (22), 3410–3416.
36. Stefanovic, B., Manojlovic, Z., Vied, C., Badger, C.D., (2019). Discovery and evaluation of inhibitor of LARP6 as specific antifibrotic compound. *Sci. Rep.*, **9**, 326–340.
37. Stefanovic, B., Michaels, H.A., Nefzi, A., (2021). Discovery of a lead compound for specific inhibition of type I collagen production in fibrosis. *ACS Med. Chem. Lett.*, **12** (3), 477–484.
38. He, T.C., Zhou, S., da Costa, L.T., Yu, J., Kinzler, K.W., Vogelstein, B., (1998). A simplified system for generating recombinant adenoviruses. *Proc. Natl. Acad. Sci. USA*, **95** (5), 2509–2514.
39. Ouellette, M.M., McDaniel, L.D., Wright, W.E., Shay, J.W., Schultz, R.A., (2000). The establishment of telomerase-

immortalized cell lines representing human chromosome instability syndromes. *Hum. Mol. Genet.*, **9** (3), 403–411.
40. Schnabl, B., Choi, Y.H., Olsen, J.C., Hagedorn, C.H., Brenner, D.A., (2002). Immortal activated human hepatic stellate cells generated by ectopic telomerase expression. *Lab. Invest.*, **82** (3), 323–333.
41. Ran, F.A., Hsu, P.D., Wright, J., Agarwala, V., Scott, D.A., Zhang, F., (2013). Genome engineering using the CRISPR-Cas9 system. *Nat. Protoc.*, **8** (11), 2281–2308.
42. Stephens, S.B., Dodd, R.D., Lerner, R.S., Pyhtila, B.M., Nicchitta, C.V., (2008). Analysis of mRNA partitioning between the cytosol and endoplasmic reticulum compartments of mammalian cells. *Methods Mol. Biol.*, **419**, 197–214.
43. Zhang, Y., Stefanovic, B., (2017). mTORC1 phosphorylates LARP6 to stimulate type I collagen expression. *Sci. Rep.*, **7**, 41173.
44. Achterberg, V.F., Buscemi, L., Diekmann, H., Smith-Clerc, J., Schwengler, H., Meister, J.-J., Wenck, H., Gallinat, S., Hinz, B., (2014). The nano-scale mechanical properties of the extracellular matrix regulate dermal fibroblast function. *J, Invest. Dermatol.*, **134** (7), 1862–1872.
45. Jia, Y., Wang, Y., Niu, L., Zhang, H., Tian, J., Gao, D., Zhang, X., Lu, T.J., Qian, J., Huang, G., Xu, F., (2021). The plasticity of nanofibrous matrix regulates fibroblast activation in fibrosis. *Adv Healthc Mater*, **10** (8), 2001856.
46. Friedman, S.L., Rockey, D.C., McGuire, R.F., Maher, J.J., Boyles, J.K., Yamasaki, G., (1992). Isolated hepatic lipocytes and Kupffer cells from normal human liver: morphological and functional characteristics in primary culture. *Hepatology*, **15** (2), 234–243.
47. McKeehan, W., Hardesty, B., (1969). The mechanism of cycloheximide inhibition of protein synthesis in rabbit reticulocytes. *Biochem. Biophys. Res. Commun.*, **36** (4), 625–630.
48. Aviner, R., (2020). The science of puromycin: From studies of ribosome function to applications in biotechnology. *Comput. Struct. Biotechnol. J.*, **18**, 1074–1083.
49. Cai, L., Fritz, D., Stefanovic, L., Stefanovic, B., (2010). Binding of LARP6 to the conserved 5' stem-loop regulates translation of mRNAs encoding type I collagen. *J. Mol. Biol.*, **395** (2), 309–326.
50. Zhang, Z., Luo, S., Barbosa, G.O., Bai, M., Kornberg, T.B., Ma, D.K., Chisholm, A.D., (2021). The conserved transmembrane protein TMEM-39 coordinates with COPII to promote collagen secretion and regulate ER stress response. *PLoS Genet.*, **17** (2), e1009317.
51. Hau, H.T.A., Ogundele, O., Hibbert, A.H., Monfries, C.A.L., Exelby, K., Wood, N.J., Nevarez-Mejia, J., Carbajal, M.A., Fleck, R.A., Dermit, M., Mardakheh, F.K., Williams-Ward, V.C., Pipalia, T.G., Conte, M.R., Hughes, S.M., (2020). Maternal Larp6 controls oocyte development, chorion formation and elevation. *Development*, **147** (4)
52. DiChiara, A.S., Li, R.C., Suen, P.H., Hosseini, A.S., Taylor, R.J., Weickhardt, A.F., Malhotra, D., McCaslin, D.R., Shoulders, M.D., (2018). A cysteine-based molecular code informs collagen C-propeptide assembly. *Nat. Commun.*, **9** (1), 4206.
53. Franceschi, R.T., Iyer, B.S., Cui, Y., (1994). Effects of ascorbic acid on collagen matrix formation and osteoblast differentiation in murine MC3T3-E1 cells. *J. Bone Miner. Res.*, **9** (6), 843–854.
54. Heinemann, F.S., Ozols, J., (1998). Isolation and structural analysis of microsomal membrane proteins. *Front. Biosci.*, **3**, d483–d493.
55. Pool, M.R., (2009). A trans-membrane segment inside the ribosome exit tunnel triggers RAMP4 recruitment to the Sec61p translocase. *J. Cell Biol.*, **185** (5), 889–902.
56. Potter, M.D., Nicchitta, C.V., (2000). Ribosome-independent regulation of translocon composition and Sec61alpha conformation. *J. Biol. Chem.*, **275** (3), 2037–2045.
57. Lu, Y., Kamel-El Sayed, S.A., Wang, K., Tiede-Lewis, LeAnn.M., Grillo, M.A., Veno, P.A., Dusevich, V., Phillips, C.L., Bonewald, L.F., Dallas, S.L., (2018). Live imaging of type I collagen assembly dynamics in osteoblasts stably expressing GFP and mCherry-tagged collagen constructs. *J. Bone Miner. Res.*, **33** (6), 1166–1182.
58. Dehm, P., Prockop, D.J., (1972). Time lag in the secretion of collagen by matrix-free tendon cells and inhibition of the secretory process by colchicine and vinblastine. *BBA*, **264** (2), 375–382.
59. Arguello, R.J., Reverendo, M., Mendes, A., Camosseto, V., Torres, A.G., Ribas de Pouplana, L., van de Pavert, S.A., Gatti, E., Pierre, P., (2018). SunRiSE - measuring translation elongation at single-cell resolution by means of flow cytometry. *J. Cell Sci.*, **131** (10)
60. Doyle, S.A., Smith, B.D., (1998). Role of the pro-alpha2(I) COOH-terminal region in assembly of type I collagen: disruption of two intramolecular disulfide bonds in pro-alpha2(I) blocks assembly of type I collagen. *J. Cell. Biochem.*, **71** (2), 233–242.
61. Buevich, A.V., Silva, T., Brodsky, B., Baum, J., (2004). Transformation of the mechanism of triple-helix peptide folding in the absence of a C-terminal nucleation domain and its implications for mutations in collagen disorders. *J. Biol. Chem.*, **279** (45), 46890–46895.
62. Bächinger, H.P., (1987). The influence of peptidyl-prolyl cis-trans isomerase on the in vitro folding of type III collagen. *J. Biol. Chem.*, **262** (35), 17144–17148.
63. Beck, K., Boswell, B.A., Ridgway, C.C., Bächinger, H.P., (1996). Triple helix formation of procollagen type I can occur at the rough endoplasmic reticulum membrane. *J. Biol. Chem.*, **271** (35), 21566–21573.
64. Lekszas, C., Foresti, O., Raote, I., Liedtke, D., Konig, E.M., Nanda, I., Vona, B., De Coster, P., Cauwels, R., Malhotra, V., Haaf, T., (2020). Biallelic TANGO1 mutations cause a novel syndromal disease due to hampered cellular collagen secretion. *Elife*, **9**
65. Saito, K., Chen, M., Bard, F., Chen, S., Zhou, H., Woodley, D., Polischuk, R., Schekman, R., Malhotra, V., (2009). TANGO1 facilitates cargo loading at endoplasmic reticulum exit sites. *Cell*, **136** (5), 891–902.
66. Li, Y., Ho, D., Meng, H., Chan, T.R., An, B., Yu, H., Brodsky, B., Jun, A.S., Michael Yu, S., (2013). Direct detection of collagenous proteins by fluorescently labeled collagen mimetic peptides. *Bioconjug. Chem.*, **24** (1), 9–16.
67. Mizuno, K., Boudko, S.P., Engel, J., Bächinger, H.P., (2010). Kinetic hysteresis in collagen folding. *Biophys. J.*, **98** (12), 3004–3014.
68. Keshwani, N., Banerjee, S., Brodsky, B., Makhatadze, G.I., (2013). The role of cross-chain ionic interactions for the stability of collagen model peptides. *Biophys. J.*, **105** (7), 1681–1688.
69. Ishikawa, Y., Bächinger, H.P., (2013). A molecular ensemble in the rER for procollagen maturation. *BBA*, **1833** (11), 2479–2491.